SSVEP-EEG Feature Enhancement Method Using an Image Sharpening Filter

Wenqiang Yan, Guanghua Xu, *Member, IEEE*, Yuhui Du, and Xiaobi Chen

***Abstract*— Steady-state visual evoked potential (SSVEP) is widely used in brain computer interface (BCI), medical detection, and neuroscience, so there is significant interest in enhancing SSVEP features via signal processing for better performance. In this study, an image processing method was combined with brain signal analysis and a sharpening filter was used to extract image details and features for the enhancement of SSVEP features. The results demonstrated that sharpening filter could eliminate the SSVEP signal trend term and suppress its low-frequency component. Meanwhile, sharpening filter effectively enhanced the signal-to-noise ratios (SNRs) of the single-channel and multi-channel fused signals. Image sharpening filter also significantly improved the recognition accuracy of canonical correlation analysis (CCA), filter bank canonical correlation analysis (FBCCA), and task-related component analysis (TRCA). The tools developed here effectively enhanced the SSVEP signal features, suggesting that image processing methods can be considered for improved brain signal analysis.**

***Index Terms*— Brain–computer interface, steady-state visual evoked potential, image sharpening filter, feature enhancement, spectrum analysis.**

I. Introduction

WHEN human eyes are stimulated by an external stimulus applied at constant frequency, the brain will generate a response with the same frequency as the external stimulus or its harmonics. This natural response to visual stimulation can be measured by voltage on the scalp, i.e., steady-state visual evoked potential (SSVEP). The amplitude of SSVEP varies with the stimulus frequency, and a significant steady-state response can be observed up to 90 Hz with optical stimulation of frequency ranging from 1-100 Hz [1]. Overall, the amplitude of SSVEP decreases as the stimulation frequency increases with specific resonance peaks for different frequency bands. Although SSVEP originates from repetitive stimulation with constant intensity and is more stable than spontaneous electroencephalogram (EEG), EEG signals can interfere with SSVEP, resulting in significantly different amplitudes for different subjects. Previous studies have shown that subject can adapt with increased stimulation duration, resulting in slight differences in SSVEP amplitude measured before and after stimulation [2]. This indicated high stability of SSVEP. Overall, the generation mechanism of SSVEP remains poorly understood. Burkitt *et al.* investigated the amplitude and phase distribution of SSVEP and found that SSVEP exhibits characteristics of both traveling and standing waves [3]. Thorpe *et al.* used EEG and magnetoencephalogram (MEG) and similarly concluded that SSVEP has characteristics of both traveling and standing waves [4]. Therefore, wave theory can be used to explain the origin of SSVEP. Some researchers have suggested that SSVEP may be related to spontaneous background EEG activities. Birca *et al.* found that intermittent photic stimulation (IPS) inhibits or desynchronizes the dominant frequency activity of the posterior brain region in the resting state for both children and adults [5], with this inhibitory effect positively related to the amplitude of SSVEP. Thus, the desynchronization of spontaneous EEG activities under IPS is related to SSVEP. Using IPS, Lazarev *et al.* reported that the amplitude spectrum of SSVEP at eleven frequencies is positively correlated with the energy spectrum in the resting state, and the amplitude spectra of the second and third harmonics are positively correlated with that of the fundamental frequency [6]. These findings verified the resonance of SSVEP and spontaneous EEG activities.

Despite its unclear generation mechanism, SSVEP is widely used in fundamental research and engineering applications owing to its high interference resistance. The most well-known application of SSVEP is in brain-computer interface (BCI) systems [7]–[10]. In BCI systems based on SSVEP, a series of optical flashing modules with different frequencies were employed as stimuli, where each stimulus corresponds to a single operation command. When the user gazes at one of the stimuli, cortical activity is modulated and a periodic rhythm with the same frequency as the stimulus or its harmonic is generated, mainly in the occipital region of the cortex. By identifying the peak frequency of the evoked EEG signal, we can identify the target that the user is gazing at, thus identifying the intention of the user.

Manuscript received November 2, 2021; revised December 25, 2021; accepted January 10, 2022. Date of publication January 13, 2022; date of current version January 28, 2022. This work was supported in part by the National Natural Science Foundation of China (NSFC) under Grant 52105308, in part by the Fundamental Research Funds for the Central Universities under Grant xhj032021010-02, and in part by the China National Post-Doctoral Program for Innovative Talents under Grant BX20200273. *(Corresponding author: Wenqiang Yan.)*

This work involved human subjects or animals in its research. Approval of all ethical and experimental procedures and protocols was granted by the Research Ethics Committee of Tsinghua University.

Wenqiang Yan and Guanghua Xu are with the State Key Laboratory for Manufacturing Systems Engineering, School of Mechanical Engineering, Xi'an Jiaotong University, Xi'an 710049, China (e-mail: yanwenq@xjtu.edu.cn).

Yuhui Du and Xiaobi Chen are with the School of Mechanical Engineering, Xi'an Jiaotong University, Xi'an 710049, China.

Digital Object Identifier 10.1109/TNSRE.2022.3142736

Recently developed algorithms related to SSVEP have focused on the effective identification of the targets of users. Examples include canonical correlation analysis (CCA) [11], filter bank canonical correlation analysis (FBCCA) [12], multivariable synchronization index (MSI) [13], likelihood ratio test (LRT) [14], individual template-based canonical correlation analysis (IT-CCA) [15], combined-canonical correlation analysis (Combined-CCA) [16], multi-way canonical correlation analysis (MwayCCA) [17], multi-set canonical correlation analysis (MestCCA) [18] and task-related component analysis (TRCA) [7]. Most of these algorithms have been designed for the application of SSVEP in BCI and aim to identify a stimulus target. In addition to BCI, SSVEP has been applied in medical detection and cognitive neuroscience as a frequency marker of brain activities. Zheng *et al.* accurately and objectively measured visual dysfunction based on different response characteristics of SSVEP between color blind/weak patients and healthy people [19]. Spiegel *et al.* explored the binocular competition mechanism of autistic patients based on SSVEP measurement, finding that the severity of autism symptoms and the diagnostic status of correctly classified individuals (autistic and control group) could be predicted solely based on neural data [20]. Additionally, SSVEP has been applied in clinical detections of aging, migraine, schizophrenia, epilepsy, and depression [21]–[24]. SSVEP has also been applied in cognitive neuroscience studies. Giani *et al.* used SSVEP to examine information integration and found integrations within vision or auditory sensations, but not between these sensations [25]. Andersen and Mueller investigated the selective attention mechanism of visual processing using SSVEP and demonstrated that the enhancement of the attended stimulus may cause the suppression of the unattended stimulus [26]. When SSVEP signals are applied for medical detection or neuroscience, the stimulus target is fixed and the amplitude or signal-to-noise ratio (SNR) at the fixed frequency is typically analyzed based on power spectra [19]–[23], [25], [26]. However, the amplitude of EEG signals is at the microvolt level, and other physiological or non-physiological (e.g., spatial electromagnetic noises) signals can interfere with these signals. As a result, amplitude and SNR of SSVEP signals are weak and difficult to extract, limiting research, analysis, and application of brain signals. Therefore, it is of great theoretical and practical significance to develop a signal processing method to effectively enhance SSVEP features.

During signal processing, EEG signals can be analyzed as images. First, EEG signals are acquired from multiple electrode channels to generate a two-dimensional matrix with the same data dimension as the image. Second, the image is a signal that varies with spatial axis x/y. For multi-channel EEG signals, each electrode channel is a signal that changes with time t and with extremely strong correlations between electrode channels. This may be because the signals recorded during EEG acquisition result from common discharges by neuron groups in human brain. The brain discharges in all directions and signals reach the scalp surface after attenuation via the folds of cortex, brain effusion, skull, and other tissues. For this reason, the brain signals collected by each electrode are the aggregated signals of various discharge sources in the brain and signals collected by different electrodes may results from discharge from the same source in the brain. Therefore, it makes sense that multi-channel EEG signals can be analyzed as image signals associated with both the x and y directions of the spatial axis. In a previous study, we proposed an image filtering denoising (IFD) method for SSVEP based on image filtering (e.g., Gaussian filtering, non-local mean filtering) [27]. First, image filtering of the multi-channel EEG signal is conducted to obtain the noise signal and then the denoised signal is obtained by subtracting this noise from the original signal. Using the IFD method, fuzzy information of the image was first obtained and detailed information is determined by subtracting this fuzzy information. Unlike the IFD method, the proposed method applies an image processing method that directly obtains the detailed information of the image for the enhancement of SSVEP features. The use of a sharpening filter based on spatial differential operation is an effective method to extract image details as it can enhance detail and contour of the image by use of a differential operator. Therefore, the image sharpening filter was applied for SSVEP signal analysis, and the signal enhancement by Prewitt, Sobel, and Laplace operators were compared. Additionally, the enhancement efficiencies of the sharpening filter on single-channel SNR and SNR after multi-channel signal fusion were verified using a public data set. The improvement effects of the sharpening filter on the recognition accuracy of the SSVEP signal were also been analyzed. These results can facilitate the improved analysis of SSVEP for BCI, medical detection and neuroscience applications.

The organization of this manuscript is as follows. In Section II, the data and methods used in this study are introduced. Section III analyzes the enhancement effect of image sharpening filtering on SSVEP signals. Discussions of the results and suggestions for future work are presented in Section IV, and our conclusions are presented in Section V.

II. Methods

A. Data Used in This Study

The enhancement effect of image sharpening filtering on SSVEP signals was verified by analyzing the SSVEP public dataset [28]. This dataset is freely available on http://bci.med.tsinghua.edu.cn/download.html. This dataset includes SSVEP-BCI recordings of 35 healthy subjects focusing on 40 characters flickering at different frequencies (8-15.8 Hz with an interval of 0.2 Hz). For each subject, the experiment consisted of six blocks, where each block contained 40 trials corresponding to all 40 characters presented in a random order. The length of each trial is 5 s, and the sampling frequency of the data is 250 Hz. Detailed description of the dataset can be found in reference [28]. The SSVEP signal analysis channels selected in this study were O_1, O_2, Oz, PO_3, PO_4, POz, PO_5, and PO_6.

B. Sharpening Filter

1) Prewitt and Sobel Operator Filters Based on First Order Differential Operation: The objective of the image sharpening filter is to highlight edges and contours. In an image, an edge

is considered to be located at a pixel with relatively large first-order differential. Therefore, edges and details can be enhanced by calculating the first-order differential of the image. In image processing, the first-order differential can be calculated by the gradient magnitude. For an image f, the gradient at coordinates (x, y) is defined as a two-dimensional column vector:

$$G[f(x,y)] = [f'_x f'_y] = [\frac{\partial f(x,y)}{\partial x} \frac{\partial f(x,y)}{\partial y}] \tag{1}$$

The vector has key geometric features, and identifies the direction of the maximum changing rate of f at (x, y). The magnitude of gradient $G[f(x, y)]$ can be expressed as $G_M[f(x, y)]$:

$$G_M[f(x,y)] = \sqrt{f'^2_x + f'^2_y} \tag{2}$$

$G_M[f(x, y)]$ is a gradient image and is generated when the x and y of all pixel positions in f are allowed to change. Therefore, it has the same dimensions as the original image. In practical applications, however, the square and square root operations in Eq (2) are approximately replaced by absolute values to simplify calculation:

$$G_M[f(x,y)] \approx |f'_x| + |f'_y| \tag{3}$$

In the calculation of digital images, derivative operation is usually approximated by differential operation. In other words, f_x' and f_y' can be expressed as:

$$f'_x = f(x,y) - f(x+1,y) \tag{4}$$
$$f'_y = f(x,y) - f(x,y+1) \tag{5}$$

Eqs (4) and (5) can be solved by filtering of image $f(x, y)$ using the templates shown in Fig. 1-A. The partial derivatives obtained using these templates are introduced into Eq (3) to determine the gradient magnitude of the image, namely the sharpening filtered image. Herein, the filter template used to calculate the gradient derivatives is denoted as the gradient operator. Gradient derivatives obtained using different gradient operators are different, resulting in the development of Prewitt and Sobel operators.

The gradient can be calculated using the Prewitt operator. Specifically, the average was first obtained, and then the difference was calculated:

$$f'_x = f(x-1,y+1) + f(x,y+1) + f(x+1,y+1) - f(x-1,y-1) - f(x,y-1) - f(x+1,y-1) \tag{6}$$

$$f'_y = f(x+1,y-1) + f(x+1,y) + f(x+1,y+1) - f(x-1,y-1) - f(x-1,y) - f(x-1,y+1) \tag{7}$$

Fig. 1-B shows the filter template corresponding to the Prewitt operator. Based on the Prewitt operator, the Sobel operator includes weighting. To do this, the impact of an adjacent point on the current pixel is dependent on the distance between the points: the impact increases as the distance decreases. Using the Sobel operator, the weighted relative values of current row/column were determined and their average and difference were calculated:

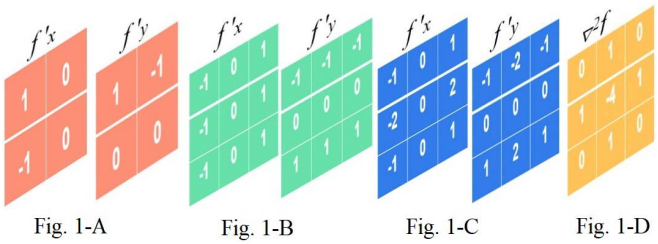

Fig. 1. Fig. 1-A. Difference operator filter template. Fig. 1-B. Prewitt operator filter template. Fig. 1-C. Sobel operator filter template. Fig. 1-D. Laplace operator filter template.

$$f'_x = f(x-1,y+1) + 2f(x,y+1) + f(x+1,y+1) - f(x-1,y-1) - 2f(x,y-1) - f(x+1,y-1) \tag{8}$$

$$f'_y = f(x+1,y-1) + 2f(x+1,y) + f(x+1,y+1) - f(x-1,y-1) - 2f(x-1,y) - f(x-1,y+1) \tag{9}$$

Fig. 1-C shows the filter template corresponding to the Sobel operator. The sharpening filtered image can be obtained by calculating the image f using the Prewitt operator or the Sobel operator by Eq (3).

2) Laplace Operator Filter Based on Second-Order Differential Operation: An alternative method for sharpening filtering is the extraction of details and edges of an image by second-order differential operation of the image. Herein, the Laplace operator is most commonly used for second-order differential operation. The Laplace operator of image f at point (x, y) is as follows:

$$\nabla^2 f(x,y) = \frac{\partial^2 f(x,y)}{\partial x^2} + \frac{\partial^2 f(x,y)}{\partial y^2} \tag{10}$$

Similar to the difference approximation used in first-order differential operation, the second-order differential can be defined as follows:

$$\frac{\partial^2 f(x,y)}{\partial x^2} = f(x+1,y) + f(x-1,y) - 2f(x,y) \tag{11}$$

$$\frac{\partial^2 f(x,y)}{\partial y^2} = f(x,y+1) + f(x,y-1) - 2f(x,y) \tag{12}$$

By substituting Eqs (11) and (12) into Eq (10), the expression of the Laplace operator can be obtained:

$$\nabla^2 f(x,y) = f(x+1,y) + f(x-1,y) + f(x,y+1) + f(x,y-1) - 4f(x,y) \tag{13}$$

Fig. 1-D shows the filter template corresponding to the Laplace operator.

C. CCA, FBCCA and TRCA Methods

When SSVEP signals are applied in BCI, the key task is the identification of the subject's target. Here, the effects of image sharpening filtering on the target recognition accuracy of SSVEP were investigated using CCA, FBCCA and TRCA as the basic algorithms.

1) CCA: For EEG data X recorded from multiple electrode leads and the reference signal Y, the goal of CCA is to find two linear projection vectors w_x and w_y so that the two groups of linear combination signals $w_x^{\mathrm{T}}X$ and $w_y^{\mathrm{T}}Y$ have the largest correlation coefficients. The canonical correlation coefficient was calculated by:

$$\rho = max \frac{E(w_x^T X Y^T w_y)}{\sqrt{E(w_x^T X X^T w_x) E(w_y^T Y Y^T w_y)}} \tag{14}$$

The reference signals Y were constructed at the stimulation frequency f:

$$Y = \left\{ \begin{array}{c} cos2\pi ft \\ sin2\pi ft \\ \cdots \\ cos2k\pi ft \\ sin2k\pi ft \end{array} \right\}, \quad t = 1/f_s, \ldots, N_s/f_s \tag{15}$$

where k is the number of harmonics, f_s is the sampling rate, and Ns represents the number of sample points. By calculating the canonical correlation coefficients between X and the reference signals at all stimulus frequencies, and the corresponding target with the maximum correlation coefficient is identified as the focused target.

2) FBCCA: As an improved version of CCA, FBCCA divides signal X into n sub-band signals through filter banks and then calculates the canonical correlation coefficient ρ_i of each sub-band signal X_i using CCA. Then, the final discrimination coefficient is determined by integration of n correlation by:

$$\tilde{\rho} = \sum_{i=1}^{n} w(i) \cdot (\rho_i)^2 \tag{16}$$

where $w(i)$ refers to the weight corresponding to the correlation coefficient of the i-th sub-band signal. This can be calculated by:

$$w(i) = i^{-a} + b, i \in [1n] \tag{17}$$

Herein, a and b are 1.25 and 0.25, respectively [12]. After obtaining integration coefficients at all stimulus frequencies, FBCCA considers the target corresponding to the maximum coefficient as the gaze target.

3) TRCA: CCA and FBCCA are training-free methods, TRCA is a training-based method, which needs to collect user training data through multiple rounds of experiments. The collected user training data is denoted as $Z \in \mathrm{R}^{Ns \times Nc \times Nf \times Nt}$, where Ns represents the number of sampling points, Nc represents the number of electrode channels, N_f represents the number of stimulation frequencies, and Nt represents the number of blocks. TRCA extracts task-related components by spatially filtering the training data. The spatial filter $w_f \in \mathrm{R}^{Nc \times 1}$ at stimulation frequency f can be calculated by the following formula:

$$\underset{w_f}{argmax} \frac{w_f^T A^T A w_f}{w_f^T B^T B w_f} \tag{18}$$

where $A \in \mathrm{R}^{Ns \times Nc}$ represents the result of averaging Nt blocks at the frequency f in Z:

$$A = \frac{1}{N_t} \sum_{i=1}^{N_t} Z_{i,f} \tag{19}$$

$B = [Z_{1,f}^T Z_{2,f}^T \ Z_{3,f}^T \ldots Z_{Nt,f}^T]^T \in R^{Nt \cdot Ns \times Nc}$, and $Z_{i,f} \in \mathrm{R}^{Ns \times Nc}$ represents the multi-channel EEG signal with stimulation frequency f in the i-th block. After calculating the spatial filter w_f at the frequency f, TRCA takes the Pearson correlation coefficient between the spatial filtered signal and the test signal $X \in \mathrm{R}^{Ns \times Nc}$ as the final discriminant coefficient:

$$p' = corr(X w_f, A w_f) \tag{20}$$

The TRCA proposed by Nakanishi et al combines the filter bank technique [7]. In this study, the filter bank technique is applied to TRCA method. After obtaining the discrimination coefficients at all stimulus frequencies, the target corresponds to the maximum coefficient as the gaze target.

D. Signal-to-Noise Ratio

The SNR was computed as the ratio between the power spectrum amplitude of a given frequency f and the average amplitude of its twenty-five surrounding neighbors ($\Delta f = 0.2\ Hz$):

$$SNR(f) = a(f) / \left\{ \frac{1}{50} \sum_{l=-25, l \neq 0}^{l=25} a(f + l \cdot \Delta f) \right\} \tag{21}$$

where $a(f)$ represents the power spectrum amplitude at the frequency f.

E. Methods for SSVEP Features Enhancement Based on Image Sharpening Filter

Fig. 2 shows the process of image sharpening filtering of SSVEP signals. Using the multi-channel signal X as the input image, the sharpening filtered signal X' can be obtained by filtering using the filter template of the selected operator (Prewitt,, Sobel, or Laplace operators) shown in Fig. 1. Sharpening filtering of the EEG signal X was achieved using *fspecial* and *imfilter*, functions from the MATLAB library. When sharpening filter is applied for spectrum analysis in medical detection and neuroscience, the sharpening filtered signal X' can be used as an analytical signal. When sharpening filter is applied for gaze target recognition in SSVEP-BCI, the sharpening filter is combined with CCA, FBCCA and TRCA methods and the SF_CCA, SF_FBCCA and SF_TRCA methods are proposed in this study. Firstly, the discriminant coefficient of the original test signal X calculated through CCA\ FBCCA\TRCA is denoted as $p_{orignal}$. Then the sharpening filter is performed on X, and the discriminant coefficient of the sharpening filtered signal X' calculated through CCA\FBCCA\TRCA is denoted as p_{SF}. The SF_CCA\SF_FBCCA\SF_TRCA method takes the integration coefficient of $p_{orignal}$ and p_{SF} as the final discriminant coefficient:

$$\hat{p} = sign(p_{orignal}) \cdot p_{orignal}^2 + sign(p_{SF}) \cdot p_{SF}^2 \tag{22}$$

where $sign\ (\cdot)$ represents the sign function.

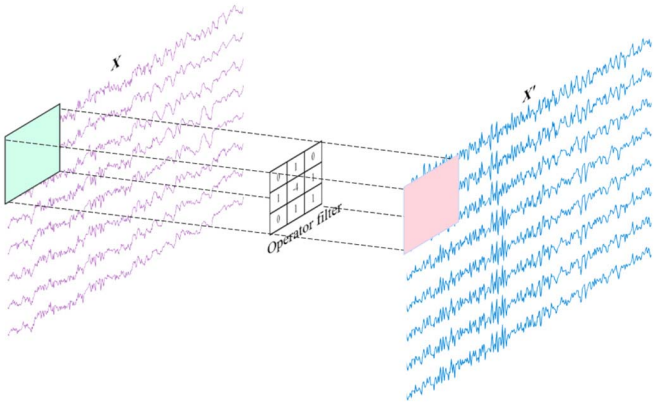

Fig. 2. The process of image sharpening filtering of SSVEP signals.

III. Results

A. Mechanism of Image Sharpening Filter Influencing SSVEP Signals

To explore how the image sharpening filtering influences SSVEP signals, we analyzed the time and frequency domains before and after application of the sharpening filter to SSVEP signals. Fig. 3-A shows the original waveform of SSVEP signals, and Fig. 3-B, 3-C and 3-D show the time domain waveforms of SSVEP signals processed by Prewitt, Sobel, and Laplace operator filters, respectively. As shown, the original waveform was not stably distributed along the baseline, and instead exhibited significant fluctuations. This can be attributed to the deviation from the baseline of the collected signals, which can be caused by zero drift of the amplifier induced by temperature variation or the movement of the EEG sensor or limb. The overall signal deviation from the baseline with time is denoted as the trend term, and this term has a direct effect on signal validity. As shown in Fig. 3-B and 3-C, waveforms of SSVEP signals filtered by the Prewitt operator or by the Sobel operator were stable and effectively eliminated the trend term. However, as shown in Fig. 3-D, the Laplace operator filter had only limited effect on elimination of the trend term, as there was severe interference in electrode channels POz, PO_6, Oz, and O_2. Time domain analysis revealed that sharpening filtering based on first-order differential can effectively eliminate the trend term of SSVEP signal, while sharpening filtering based on second-order differential was not effective at elimination of the trend term of SSVEP signal.

We next analyzed the frequency domains of SSVEP signals after image sharpening filtering. Fig. 4-A illustrates the power spectra of eight electrode channels of the original signal for a signal stimulation frequency of 11 Hz. The red dots indicate the amplitude at the fundamental frequency of stimulation and its harmonic frequencies. Fig. 4-B, 4-C, and 4-D show the power spectra of SSVEP signals processed by Prewitt, Sobel, and Laplace operator filters, respectively. As shown in Fig. 4-B and 4-C, the Prewitt and Sobel operator filters exhibit high-pass filtering effects on SSVEP signals, with significant suppression of the low-frequency components of signals in the eight electrode channels. The stimulus frequency of SSVEP signals is typically set above 7 Hz. The low-frequency components of EEG signals hinders accurate analysis of SSVEP signals. According to the spectra of the original signal, the low-frequency components severely interfere with the amplitude of the effective component of the SSVEP signal. Among the eight electrode channels of the original signal, the maximum power spectrum amplitudes of signals from PO_4, PO_6, Oz, and O_2 in the effective band range of SSVEP (>7 Hz) correspond to non-stimulus frequencies, instead of the stimulus frequency. The amplitudes at the fundamental frequency of stimulus and its harmonic frequencies of signals from PO_4, PO_6, Oz and O_2 were significantly enhanced by filtering by either the Prewitt operator or the Sobel operator so that these became the maximum amplitudes in the effective frequency band, indicating that these filters effectively enhanced the frequency features of the SSVEP signals. The Laplace operator filter did not achieve the high-pass filtering of SSVEP signals. As shown in Fig. 4-D, significant interference by low-frequency components were observed in all electrode channels, especially PO_Z, weakening the amplitude at the stimulation frequency.

The results revealed that the Prewitt operator and the Sobel operator based on first-order differential operation can effectively enhance the features of SSVEP signals, while the Laplace operator based on second-order differential operation is not suitable for analysis of SSVEP signals. Additionally, Prewitt operator and Sobel operator filters can effectively eliminate the trend terms of SSVEP signals and achieve high-pass filtering by suppressing low-frequency interferences, which facilitates elimination of noises in SSVEP signal and enhancing the SNR.

B. Enhancement of SSVEP Signal Features by Image Sharpening Filter

When SSVEP signals are applied for medical detection and neuroscience, spectrum analysis is typically required for the collected EEG signals. The signals from either single-channel EEG or multi-channel EEG fused by spatial filtering can be used for specyrum analysis. In this study, the SNR was investigated for each single channel electrode signal after image sharpening of SSVEP and multi-channel EEG fused by spatial filtering. As discussed in Section III-A, the Laplace operator filter is not suitable for analysis of SSVEP signals, so the Laplace operator filter was not applied for subsequent experiments.

Fig. 5-A shows the SNR of the original signal, and Fig. 5-B and 5-C show the SNRs of the signals after sharpening filtering by the Prewitt and the Sobel operators. In this analysis, the data analysis length was 5 s and the color value reflects the SNR. To calculate the SNR of each electrode channel, the average of SNRs of six blocks of each subject was considered the SNR for that subject and the average of SNRs of 34 subjects (the data file of subject 5 in the public data set was damaged and could not be downloaded) was considered the overall result. The SNR at frequency f was calculated according to Eq (18). There SNRs of signals from PO_3, PO_z and O_z were similar before and after sharpening filtering, but the SNRs of the signals from PO_5, PO_4, PO_6 and O_2 at fundamental and double frequencies and signal from O_1

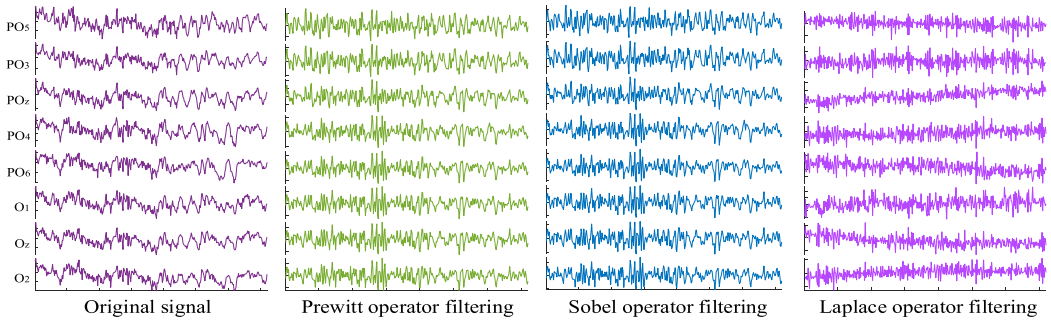

Fig. 3-A Fig. 3-B Fig. 3-C Fig. 3-D

Fig. 3. Fig. 3-A. The original waveform of SSVEP signal. Fig. 3-B. The Prewitt operator filtered waveform of SSVEP signal. Fig. 3-C. The Sobel operator filtered waveform of SSVEP signal. Fig. 3-D. The Laplace operator filtered waveform of SSVEP signal.

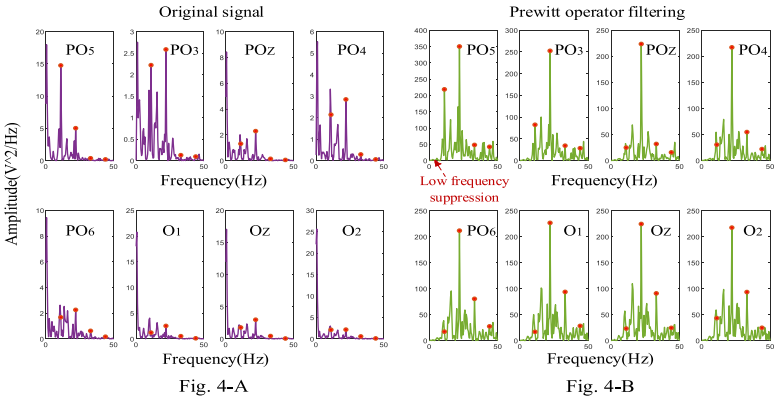

Fig. 4-A Fig. 4-B

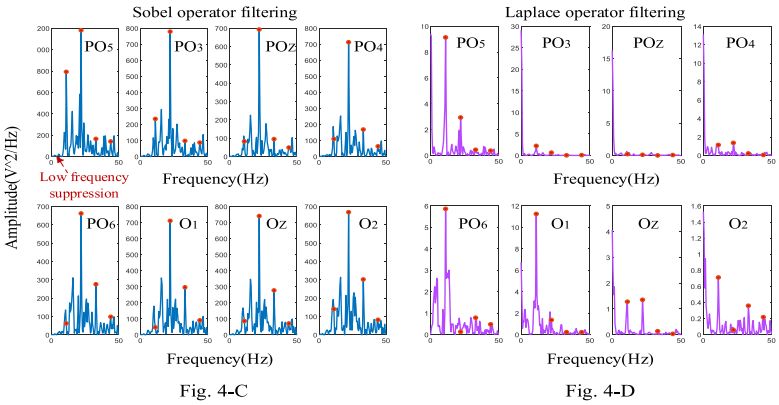

Fig. 4-C Fig. 4-D

Fig. 4. Fig. 4-A. The spectrum of original signal. Fig. 4-B. The spectrum of Prewitt operator filtered signal. Fig. 4-C. The spectrum of Sobel operator filtered signal. Fig. 4-D. The spectrum of Laplace operator filtered signal. The red dots indicate the amplitude at the fundamental frequency of stimulation and its harmonic frequencies.

at triple frequency were significantly enhanced by sharpening filtering.

Fig. 6-A, 6-B, and 6-C illustrate the SNRs of the one-dimensional signals obtained by fusion of signals from the eight electrode channels via spatial filtering (by CCA). The signals shown in Fig. 6-B and 6-C were filtered by the Prewitt and the Sobel operators, respectively, before fusion using a data length of 5 s. For the calculation of SNRs, signals from the eight channels were fused into a one-dimensional signal using the spatial filter w_x (Equation 14) as calculated by CCA, and the average SNRs of the six blocks of each subject was obtained. The average SNRs of the 34 subjects was obtained and considered the overall result. The SNR at frequency f was calculated using Eq (18). Compared with the original SSVEP signal, sharpening filtered SSVEP signals exhibited significantly enhanced SNRs at double, triple, quadruple, and quintuple frequencies. The SNRs of the original signal at quadruple and quintuple frequencies were extremely low, and those after the sharpening filtering were significantly enhanced. The fusion of multi-channel electrode signals leads to a signal with enhanced SNR compared with single-channel ones, resulting in improved accuracy of SSVEP signal analysis. Therefore, fusion of information contained in multi-electrode EEG signals improves spectrum analysis of SSVEP signals for medical detection and neuroscience.

In summary, the SNRs of both single-channel and multi-channel fused SSVEP signals were effectively enhanced by image sharpening filter, suggesting this tool could promote the accuracy of SSVEP spectrum analysis.

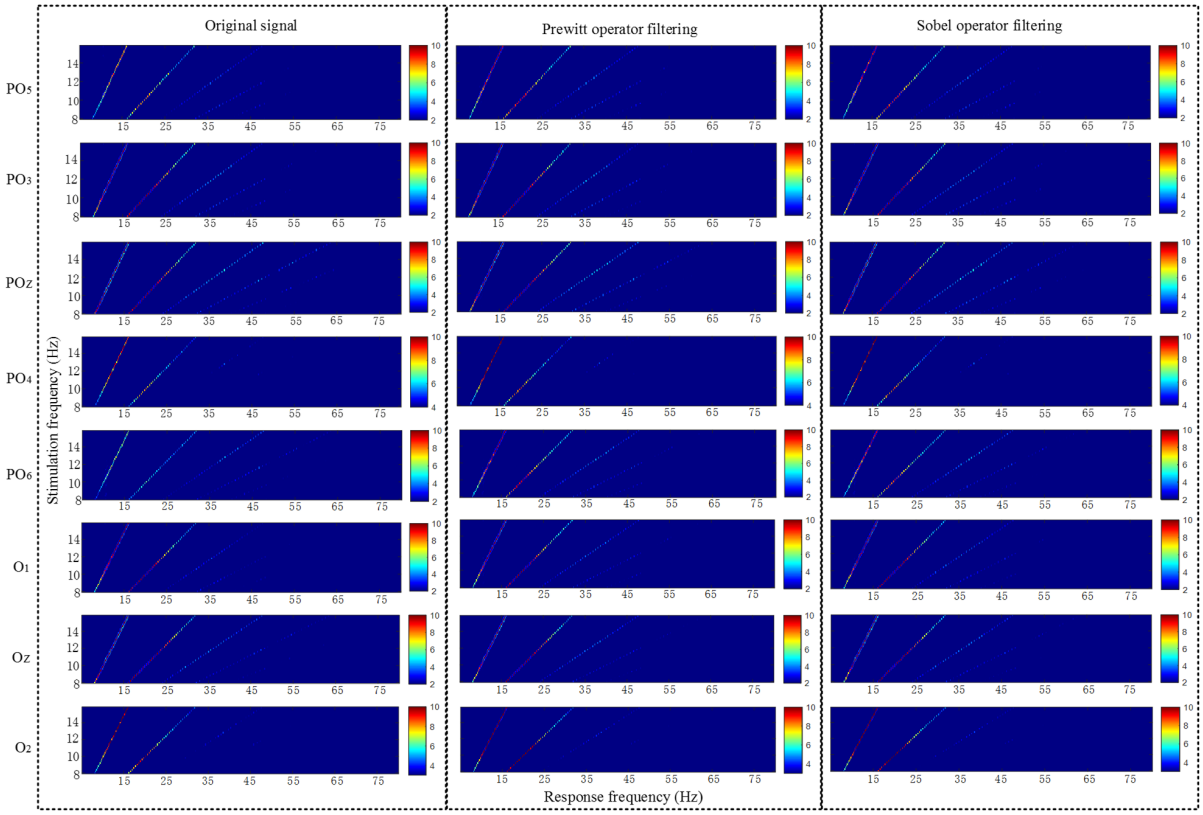

Fig. 5-A Fig. 5-B Fig. 5-C

Fig. 5. Fig. 5-A. The SNR of original signal. Fig. 5-B. The SNR of Prewitt operator filtered signal. Fig. 5-C. The SNR of Sobel operator filtered signal.

C. Effects of Image Sharpening Filter on Accuracy of SSVEP Target Recognition

Due to the visual delay of human eyes under SSVEP stimulation [29], the first 40 sampling points after the start of stimulation were removed from the SSVEP data analysis. Among them, the number of harmonics of the reference signal in CCA and FBCCA was set to 3, and the number of sub-band filters of FBCCA was set to 3. To calculate the accuracy, the recognition accuracies of six blocks of each subject were averaged and considered the recognition accuracy for each subject. The average recognition accuracy of the 34 subjects was then obtained and considered the final result. Paired-t test was used to determine significant differences (define as p <0.05) in accuracy for different methods.

Fig. 7 illustrates the recognition accuracies of CCA and SF_CCA methods, using a data analysis length of 1 - 2 s and an interval of 0.2 s. The analysis signal (for CCA is original signal X, and for SF_CCA is sharpened filter signal X') are band-pass filtered by Chebyshev filter with passband range of 8-48 Hz before using CCA and SF_CCA methods for feature recognition. As shown in Fig. 7, the SF_CCA method significantly improved the recognition accuracy of the original SSVEP signal, regardless of the stimulation duration. The accuracies of SF_CCA method obtained by the two operator filters were similar. With stimulation durations of 1, 1.2, 1.4, 1.6, 1.8, and 2 s, the recognition accuracies of SF_CCA were improved by 9.88%, 9.28%, 9.02%, 6.78%, 6.42%, and 5.4%, respectively, compared with the basic CCA algorithm. Paired t-test showed a significant difference between the accuracies of SF_CCA and basic CCA methods ($*p < 0.05$, $**p < 0.01$).

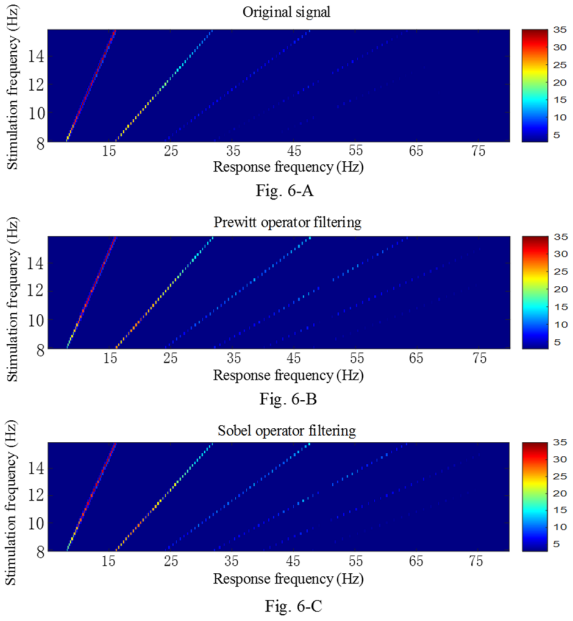

Fig. 6-A Fig. 6-B Fig. 6-C

Fig. 6. Fig. 6-A. The SNR of original multi-channel fusion signal. Fig. 6-B. The SNR of multi-channel fusion signal filtered by Prewitt operator. Fig. 6-C. The SNR of multi-channel fusion signal filtered by Sobel operator.

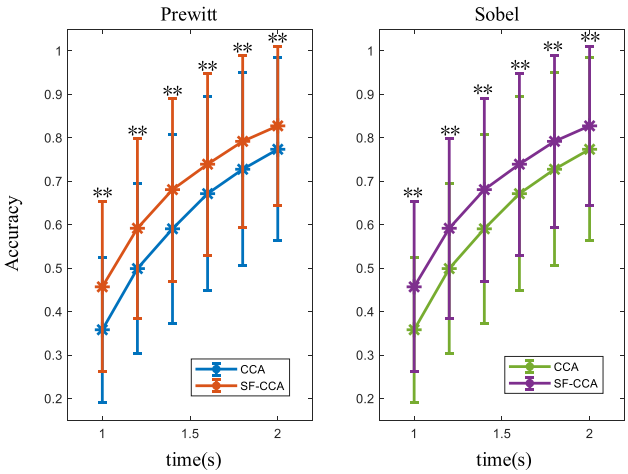

Fig. 7. The recognition accuracies of the CCA and SF-CCA methods.

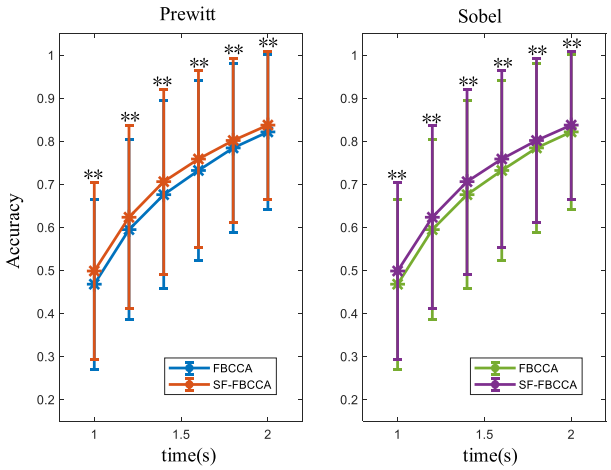

Fig. 8. The recognition accuracies of the FBCCA and SF-FBCCA methods.

Fig. 8 illustrates the recognition accuracies of FBCCA and SF_FBCCA methods. According to the filter design reported previously [12], the passband and stopband corner frequencies of the first filter bank were [6 90] and [4 100] Hz, respectively; passband and stopband corner frequencies of the second filter bank were [14 90] and [10 100] Hz, respectively; passband and stopband corner frequencies of the third filter bank were [22 90] and [16 100] Hz, respectively. As shown in Fig. 8, with stimulation durations of 1, 1.2, 1.4, 1.6, 1.8, and 2 s, the recognition accuracies of the SF-FBCCA method were improved by 3.07%, 2.87%, 3.03%, 2.65%, 1.73%, and 1.58%, respectively, compared with the basic FBCCA method. Paired t-test shows there is a significant difference between the two methods ($*p < 0.05$, $**p < 0.01$).

Fig. 9 illustrates the recognition accuracies of TRCA and SF_TRCA methods, using a data analysis length of 0.5 - 0.8 s and an interval of 0.1 s. When calculating the recognition accuracy of each subject, the leave-one-out method was used to test the recognition accuracy of six blocks in turn by using five blocks of six blocks as training data. As shown in Fig. 9, with stimulation durations of 0.5, 0.6, 0.7, and 0.8 s, the recognition accuracies of the SF-TRCA method were improved by 1.95%, 2.02%, 1.12%, and 0.85%, respectively, compared with the basic TRCA method. Paired t-test shows there is a significant

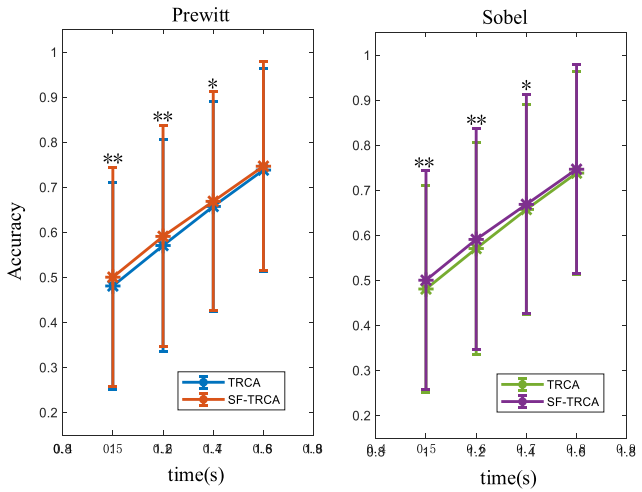

Fig. 9. The recognition accuracies of the TRCCA and SF-TRCCA methods.

difference between the two methods except for 0.8 s stimulus duration ($*p < 0.05$, $**p < 0.01$).

Overall, the application of sharpening filter in SSVEP feature recognition has a positive performance improvement effect for both CCA, FBCCA, and TRCA methods.

IV. Discussion

Enhancement of SSVEP features by signal processing is essential for the accurate analysis of SSVEP. Previous studies have used the IFD method to eliminate noise in SSVEP signals [27], suggesting that image processing can improve the analysis of SSVEP signals. Using IFD, the fuzzy information was obtained and them the detailed information was determined. Unlike IFD, the image sharpening filter can be applied to directly obtain detailed information and was applied here for SSVEP signal analysis.

First, the effects of sharpening filter on SSVEP signals were investigated. The time domain results indicate that use of a sharpening filter (with either the Prewitt operator filter or the Sobel operator filter) helps to eliminate the trend term of the signal, which limits accurate signal analysis. The elimination of the trend term by sharpening filter can enhance the features of SSVEP signals. The frequency domain results reveal that sharpening filter result in high-pass filtering of SSVEP signals, with suppression of the low-frequency components of SSVEP signals. The commonly used frequency band range of SSVEP is >7 Hz, and the low-frequency component is considered noise. Thus, the elimination of low-frequency components by sharpening filter is essentially eliminates the noise in SSVEP signals. Overall, both time domain and frequency domain analyses suggest that use of a sharpening filter enhances the features of SSVEP signals. When SSVEP signals are applied for medical detection and neuroscience, the subject's stimulus target is known, and the spectrum analysis is usually required for collected signals. Therefore, we verified that sharpening filter enhanced SNR of SSVEP signals. Analysis of SNRs of each single-channel electrode signals and multi-channel fused electrode signals after image sharpening indicate that sharpening filter effectively enhanced SNRs of SSVEP signals, which will facilitate use of these signals for medical detection and neuroscience applications. The target recognition accuracy

for use of SSVEP signals in BCI was also analyzed. The results demonstrate that the application of sharpening filter can significantly improve the recognition accuracy of CCA, FBCCA, and TRCA for any stimulation duration. Overall, the proposed image sharpening filtering method has great application potential for spectrum analysis and BCI.

Image processing can great improves analysis of SSVEP signals. In a previous study [27], noises obtained by fuzzy filtering (e.g., Gaussian filtering, mean filtering) of SSVEP signals were subtracted from the original signal. In this study, SSVEP signals were directly filtered by the image detail extraction method. Both methods have been demonstrated to enhance features of SSVEP signals. Compared with our previously proposed IFD method [27], the proposed method in this study is better for the analysis of SSVEP signals. Using IFD, the performances of CCA were enhanced by 1.64% and 3.11% for stimulus duration of 1 and 2 s, respectively [27], but the use of the sharpening filter enhanced CCA performances by 9.88% and 5.4%, respectively. Future work should focus on improvement of methods for the more accurate extraction of image edges and details.

V. Conclusion

Enhancement of SSVEP features is essential for the accurate analysis of SSVEP signals. Based on previous studies, a sharpening filtering method that is used to extract image details was applied for the analysis of SSVEP signals. The results demonstrate that the use of a sharpening filter can effectively eliminate the trend term and suppress the low frequency components of SSVEP signals. The SNRs of individual each single-channel electrode signals and the multi-channel fused electrode signal were enhanced by sharpening filter. Sharpening filter significantly improved the recognition by CCA, FBCCA, and TRCA, regardless of the stimulation duration. Overall, the results from this study indicate that sharpening filter can be beneficial for spectrum analysis and BCI. In general, image processing methods have great application potential for improved analysis of EEG signals.

References

[1] C. S. Herrmann, "Human EEG responses to 1–100 Hz flicker: Resonance phenomena in visual cortex and their potential correlation to cognitive phenomena," *Exp. Brain Res.*, vol. 137, nos. 3–4, pp. 346–353, Apr. 2001.

[2] S. P. Heinrich and M. Bach, "Adaptation dynamics in pattern-reversal visual evoked potentials," *Documenta Ophthalmol.*, vol. 102, no. 2, pp. 141–156, Mar. 2001.

[3] G. R. Burkitt, R. B. Silberstein, P. J. Cadusch, and A. W. Wood, "Steady-state visual evoked potentials and travelling waves," *Clin. Neurophysiol.*, vol. 111, no. 2, pp. 246–258, Feb. 2000.

[4] S. G. Thorpe, P. L. Nunez, and R. Srinivasan, "Identification of wave-like spatial structure in the SSVEP: Comparison of simultaneous EEG and MEG," *Statist. Med.*, vol. 26, no. 21, pp. 3911–3926, Sep. 2007.

[5] A. Birca, L. Carmant, A. Lortie, and M. Lassonde, "Interaction between the flash evoked SSVEPs and the spontaneous EEG activity in children and adults," *Clin. Neurophysiol.*, vol. 117, no. 2, pp. 279–288, Feb. 2006.

[6] V. V. Lazarev, D. M. Simpson, B. M. Schubsky, and L. C. deAzevedo, "Photic driving in the electroencephalogram of children and adolescents: Harmonic structure and relation to the resting state," *Brazilian J. Med. Biol. Res.*, vol. 34, no. 12, pp. 1573–1584, Dec. 2001.

[7] M. Nakanishi, Y. Wang, X. Chen, Y. Wang, X. Gao, and T.-P. Jung, "Enhancing detection of SSVEPs for a high-speed brain speller using task-related component analysis," *IEEE Trans. Biomed. Eng.*, vol. 65, no. 1, pp. 104–112, Jan. 2018.

[8] C. M. Wong *et al.*, "Learning across multi-stimulus enhances target recognition methods in SSVEP-based BCIs," *J. Neural Eng.*, vol. 17, no. 1, Jan. 2020, Art. no. 016026.

[9] W. Yan, G. Xu, J. Xie, M. Li, and Z. Dan, "Four novel motion paradigms based on steady-state motion visual evoked potential," *IEEE Trans. Biomed. Eng.*, vol. 65, no. 8, pp. 1696–1704, Aug. 2018.

[10] W. Yan *et al.*, "Enhancing detection of steady-state visual evoked potentials using channel ensemble method," *J. Neural Eng.*, vol. 18, no. 4, Aug. 2021, Art. no. 046008.

[11] Z. Lin, C. Zhang, W. Wu, and X. Gao, "Frequency recognition based on canonical correlation analysis for SSVEP-based BCIS," *IEEE Trans. Biomed. Eng.*, vol. 54, no. 6, pp. 1172–1176, Jun. 2007.

[12] X. Chen, Y. Wang, S. Gao, T.-P. Jung, and X. Gao, "Filter bank canonical correlation analysis for implementing a high-speed SSVEP-based brain–computer interface," *J. Neural Eng.*, vol. 12, no. 4, Aug. 2015, Art. no. 046008.

[13] Y. Zhang, P. Xu, K. Cheng, and D. Yao, "Multivariate synchronization index for frequency recognition of SSVEP-based brain-computer interface," *J. Neurosci. Meth.*, vol. 221, pp. 32–40, Jan. 2014.

[14] Y. Zhang, L. Dong, R. Zhang, D. Yao, Y. Zhang, and P. Xu, "An efficient frequency recognition method based on likelihood ratio test for SSVEP-based BCI," *Comput. Math. Method Med.*, vol. 2014, Aug. 2014, Art. no. 908719.

[15] M. Nakanishi, Y. Wang, Y.-T. Wang, and T.-P. Jung, "A comparison study of canonical correlation analysis based methods for detecting steady-state visual evoked potentials," *PLoS ONE*, vol. 10, no. 10, Oct. 2015, Art. no. e0140703.

[16] M. Nakanishi, Y. J. Wang, Y. T. Wang, Y. Mitsukura, and T. P. Jung, "A high-speed brain speller using steady-state visual evoked potentials," *Int. J. Neural Syst.*, vol. 24, no. 6, pp. 1–19, Sep. 2014.

[17] Y. Zhang *et al.*, "Multiway canonical correlation analysis for frequency components recognition in SSVEP-based BCIs," in *Proc. 18th Int. Conf. Neural Inf. Process. (ICONIP)*. Berlin, Germany: Springer, Nov. 2011, pp. 95–287.

[18] Y. Zhang, G. Zhou, J. Jin, X. Wang, and A. Cichocki, "Frequency recognition in SSVEP-based BCI using multiset canonical correlation analysis," *Int. J. Neural Syst.*, vol. 24, no. 4, pp. 1–14, 2014.

[19] X. Zheng *et al.*, "Real-time, precise, rapid and objective visual acuity assessment by self-adaptive step SSVEPs," *J. Neural Eng.*, vol. 18, no. 4, Aug. 2021, Art. no. 046047.

[20] A. Spiegel, J. Mentch, A. J. Haskins, and C. E. Robertson, "Slower binocular rivalry in the autistic brain," *Current Biol.*, vol. 29, no. 17, pp. 2948–2953, 2019.

[21] H. Macpherson, A. Pipingas, and R. Silberstein, "A steady state visually evoked potential investigation of memory and ageing," *Brain Cognition*, vol. 69, no. 3, pp. 571–579, Apr. 2009.

[22] K. Shibata, K. Yamane, K. Otuka, and M. Iwata, "Abnormal visual processing in migraine with aura: A study of steady-state visual evoked potentials," *J. Neurol. Sci.*, vol. 271, nos. 1–2, pp. 119–126, Aug. 2008.

[23] G. P. Krishnan *et al.*, "Steady state visual evoked potential abnormalities in schizophrenia," *Clin. Neurophysiol.*, vol. 116, no. 3, pp. 614–624, Mar. 2005.

[24] G. Harding, A. J. Wilkins, G. Erba, G. L. Barkley, and R. S. Fisher, "Photic- and pattern-induced seizures: Expert consensus of the epilepsy foundation of America working group," *Epilepsia*, vol. 46, no. 9, pp. 1423–1425, Sep. 2005.

[25] A. S. Giani, E. Ortiz, P. Belardinelli, M. Kleiner, H. Preissl, and U. Noppeney, "Steady-state responses in MEG demonstrate information integration within but not across the auditory and visual senses," *NeuroImage*, vol. 60, no. 2, pp. 1478–1489, Apr. 2012.

[26] S. K. Andersen and M. M. Müller, "Behavioral performance follows the time course of neural facilitation and suppression during cued shifts of feature-selective attention," *Proc. Nat. Acad. Sci. USA*, vol. 107, no. 31, pp. 13878–13882, Aug. 2010.

[27] W. Q. Yan, C. H. Du, Y. C. Wu, X. W. Zheng, and G. H. Xu, "SSVEP-EEG denoising via image filtering methods," *IEEE Trans. Neural Syst. Rehabil. Eng.*, vol. 29, pp. 1634–1643, 2021.

[28] Y. Wang, X. Chen, X. Gao, and S. Gao, "A benchmark dataset for SSVEP-based brain–computer interfaces," *IEEE Trans. Neural Syst. Rehabil. Eng.*, vol. 25, no. 10, pp. 1746–1752, Oct. 2017.

[29] X. Chen, Y. Wang, M. Nakanishi, X. Gao, T.-P. Jung, and S. Gao, "High-speed spelling with a noninvasive brain–computer interface," *Proc. Nat. Acad. Sci. USA*, vol. 112, no. 44, pp. E6058–E6067, Nov. 2015.